Environmental Research 282 (2025) 122082

Contents lists available at ScienceDirect

Environmental Research

journal homepage: www.elsevier.com/locate/envres

Chemometric discrimination of airborne fibres: microplastics, regenerated cellulose and natural fibres

Carlos Edo [a,*,1], Marica Erminia Schiano [b], Sergio J. Álvarez-Méndez [c], Javier Hernández-Borges [d,e], Daura Vega-Moreno [f], Ana Molina-Rodríguez [f], May Gómez [g], Alicia Herrera [g], Miguel González-Pleiter [h,i], Francisca Fernández-Piñas [h,i], Roberto Rosal [a]

[a] Department of Chemical Engineering, Universidad de Alcalá, Alcalá de Henares, E-28871, Madrid, Spain
[b] Dipartimento di Farmacia, Università Degli Studi di Napoli Federico II, Via D. Montesano, 49, I-80131, Naples, Italy
[c] Departamento de Química Orgánica, Universidad de La Laguna, Avda. Astrofísico Fco. Sánchez, s/n°, 38206, San Cristóbal de La Laguna, Tenerife, Spain
[d] Departamento de Química, Unidad Departamental de Química Analítica, Facultad de Ciencias Universidad de La Laguna (ULL), Avda. Astrofísico Fco. Sánchez, s/n, 38206, San Cristóbal de La Laguna, Spain
[e] Instituto Universitario de Enfermedades Tropicales y Salud Pública de Canarias, Universidad de La Laguna (ULL), Avda. Astrofísico Fco. Sanchéz, s/n, 38206, San Cristóbal de La Laguna, Spain
[f] Departamento de Química, Universidad de Las Palmas de Gran Canaria (ULPGC), Spain
[g] Ecophysiology of Marine Organisms (EOMAR), IU-ECOAQUA, Universidad de Las Palmas de Gran Canaria, Canary Islands, 35017, Las Palmas de Gran Canaria, Spain
[h] Department of Biology, Faculty of Science, Universidad Autónoma de Madrid, 28049, Madrid, Spain
[i] Centro de Investigación en Biodiversidad y Cambio Global (CIBC-UAM), Universidad Autónoma de Madrid, 28049, Madrid, Spain

ARTICLE INFO

Keywords:
Airborne fibres
Cellulose fibres
Microplastics
OPLS-DA
Indoor environment
Outdoor environment

ABSTRACT

Interest in airborne microplastics has surged in the past decade, and a range of complementary tools are now used to characterize the different polymer found in samples. Most surveys, however, focus almost exclusively on synthetic fragments and fibres, overlooking the cellulosic fraction that often dominates particle counts. In this study, we measured the concentration of airborne particles in a range of indoor and outdoor settings and including densely populated areas, industrial zones, insular locations and natural reserve areas. We quantified both number- and mass-based concentrations of microplastics (MPs) and cellulosic fibres (CFs), with the latter outnumbering MPs by at least one order of magnitude. The average plastic-particle load was 0.024 MP/m^3 (0.007–0.043 MP/m^3), whereas no MPs were detected in the natural reserve. MPs consisted mainly of polyethylene, acrylic and polypropylene, while polyester fibres predominated indoors. Because cellulosic materials can be either natural debris or anthropogenic fibres, we applied an advanced chemometric workflow, discriminant analysis coupled with Hotelling distances on mid-IR spectra, to distinguish cotton/linen textiles and regenerated cellulose (viscose, modal, Tencel) from plants, cutting ambiguous assignments by more than half. Roughly 50 % of all CFs were thus traced to textile sources. These results underline the importance of including CFs in airborne-plastic assessments and demonstrate that robust, yet widely accessible, μ-FTIR chemometric methods can deliver the resolution needed for accurate exposure and risk evaluations.

1. Introduction

Over 400 million tons of plastic are produced annually, with an average growth rate of over 2 % per year in the past decade (PlasticsEurope, 2023). Despite slower production growth in some developed countries, 52.1 million tons of plastic waste are mismanaged annually, polluting the environment (Cottom et al., 2024). Global concerns about plastic pollution have surged in recent years, but plastic debris have been documented in the environment for decades (Gündoğdu et al., 2024; Napper and Thompson, 2020). Synthetic

* Corresponding author. Department of Analytical Chemistry, Physical Chemistry and Chemical Engineering, Universidad de Alcalá, E-28871, Madrid, Spain.
E-mail address: carlos.edo@snm.ku.dk (C. Edo).
[1] Current address: Natural History Museum of Denmark, University of Copenhagen, Copenhagen, Denmark.

https://doi.org/10.1016/j.envres.2025.122082
Received 21 April 2025; Received in revised form 23 May 2025; Accepted 3 June 2025
Available online 4 June 2025

polymers often co-occur with semi-synthetic materials like textile fibres, sharing similar characteristics and risks. Anthropogenic fibres, including plastics and processed materials, are significant pollutants. Annually, an estimated 200,000 to 500,000 tons of textile-derived microplastics (MPs) enter marine ecosystems globally (European Environment Agency, 2022).

Fibres are particularly relevant in the atmosphere, a relatively new area of study that has received far less attention compared to the marine environment. Due to their greater air resistance relative to their weight, fibres experience lower settling velocities, enabling them to remain suspended in the air for extended periods (González-Pleiter et al., 2021; Xiao et al., 2023). This is the main reason why fibres are the dominant shape in outdoor and indoor air (Ageel et al., 2024; Edo et al., 2023). This is also why the atmosphere plays a crucial role in the long-range transport of microplastic fibres, a term that should not be confused with 'microfibres', which has a specific technical meaning that generally refers to fibres with a linear density of 1 dtex or less (Miraftab, 2000).

The occurrence of atmospheric microplastic fibres has been reported in various studies worldwide (D. Luo et al., 2024; O'Brien et al., 2023; Zhao et al., 2023). Along with synthetic polymers, some studies report a high number of cellulosic fibres, which can be either natural (e.g., plant remains) or anthropogenic, the latter including textile fibres (Finnegan et al., 2022; Stanton et al., 2019). Even native cellulosic fibres, when transformed into fabrics, undergo chemical or mechanical treatments that often include the addition of a variety of additives, such as softeners, anti-wrinkle agents, colour fixatives, flame retardants, and dyes (Darbra et al., 2012). Furthermore, there is a category of semisynthetic materials made from regenerated cellulose that includes Viscose (or Rayon), Tencel (or Lyocell), and Modal (Parajuli et al., 2021).

A wide array of spectroscopic and thermo-analytical techniques is now used to chemically identify those mentioned airborne fibres, both natural and synthetic from diverse matrices. Most studies still rely on optical microscopy combined with μ-FTIR, a non-destructive method supported by extensive reference libraries but limited by a diffraction-controlled spatial resolution of ≈10 μm and relatively long scan times (Tarte et al., 2024). Throughput can be increased with Focal Plan Array (FPA-μ-FTIR), which collects hundreds of spectra per second across the full mid-IR window (4000-650 cm^{-1}) yet retains the same practical size limit (~10 μm) ((Y. Liu et al., 2025; Simon et al., 2018). Other alternative is Laser Direct Infrared (LDIR) imaging, driven by quantum-cascade lasers, that is a powerful method that pushes the automated detection threshold down to ≈ 5 μm and analyses entire filters in minutes. As a negative aspect, its spectral range is restricted to 975-1800 cm^{-1} and both equipment and available libraries are still costly and scarce (López-Rosales et al., 2025; Pagliaccia et al., 2025). On the other hand, Raman microspectroscopy offers sub-micrometre resolution and can target fibres <5 μm, although fluorescence from dyes or ageing products often masks the signal (Azari et al., 2024). A newly alternative is optical photothermal infrared microspectroscopy (O-PTIR), which couples a tuneable mid-IR source with a visible probe to deliver co-registered IR and Raman spectra at ~500 nm spatial resolution covering the whole microplastic range (Amato-Lourenço et al., 2025; Tarafdar, Xie, Gowen, O'Higgins and Xu, 2024). The problem of O-PTIR is it remains costly, and its spectral databases are nascent, limiting routine adoption. Finally, in parallel, pyrolysis-GC/MS is gaining popularity for MPs research, and this include fibres of varied composition (Dehaut et al., 2022; Käppler et al., 2018; Nacci et al., 2022). Despite its high molecular specificity, it requires rigorous pretreatment to remove matrix interferences and sacrifices size-resolved information while demanding a minimum sample mass.

This study introduces a novel approach for assessing the chemical nature of airborne fibres by coupling transmission μ-FTIR spectroscopy with advanced multivariate chemometric analysis. Through an extensive sampling campaign that included urban and natural locations as well as indoor and outdoor settings, we quantified both the number- and mass-based concentrations of microplastic fibres, with particular emphasis on cellulosic polymers, which are ubiquitous in the atmosphere yet have remained comparatively understudied. The significance of our workflow lies in its ability to bridge the gap between cutting-edge analytical platforms and instrumentation already available in many laboratories. By combining conventional μ-FTIR with chemometric techniques, we demonstrate that it is possible to discriminate natural fibres, cellulosic textiles (e.g., cotton and linen), and semisynthetic materials derived from regenerated cellulose. Our results sheds light on the composition of atmospheric fibres and indicates that anthropogenic contributions may currently be underestimated.

2. Material and methods

2.1. Sampling

To capture a broad gradient of anthropogenic material, 32 sampling sites representing diverse urban, industrial and natural settings across mainland Spain and the geographically isolated Canary Islands were selected. In each region, both indoor and outdoor samples were collected.

Outdoor air sampling was conducted at four locations in the Madrid region, including urban areas in the centre of Madrid and Alcalá de Henares, a medium-sized city in the metropolitan area of Madrid. Eight samples were collected in Tarragona, four from the industrial area of Vila-Seca and four from locations within the Ebro Delta natural reserve. Additionally, eight outdoor sites were selected in the Canary Islands: four on Tenerife, in San Cristóbal de La Laguna and Santa Cruz de Tenerife, and four on Gran Canaria, including port areas and coastal locations in Tafira and Las Palmas de Gran Canaria. Indoor samples were collected from public environments, including conference rooms, classrooms, and halls in public buildings across four locations in the Madrid region, Tenerife, and Gran Canaria. Sampling locations were selected to represent a range of environments, including urban, peri-urban, and natural areas. Details of sampling locations are provided in Supplementary Material (SM, Fig. S1 and Table S1).

Field campaigns were carried out on punctual captures from November 2023 through June 2024, scheduled only on sunny, low-wind days to ensure stable flow and reliable operation. All samples were taken at pedestrian height (~1 m) isolated from direct ground contact in both indoor and outdoor environments. Only two samples collected in Madrid were collected at rooftop level for comparison purposes. After each sampling session, the filter holder was carefully opened and the used filters together with their rings were transferred to clean glass Petri dishes for subsequent laboratory processing.

Air samples were collected with an Intex® 12 V electric air-pump, powered on-site by a portable battery. A collector adapted from a Sartorius 16254 holder was connected to the pump. This collector, made of stainless-steel filter holder was modified by adding two steel rings so it could secure two 25 μm-pore stainless-steel filters (Ø47 mm), thereby maximizing retention and preventing the loss of long fibres (Fig. 1). Laboratory calibration with a hot-wire anemometer confirmed a steady airflow of approximately 90 m^3/h, meaning each replicate captured 50 m^3 of air in roughly 30 min. Three replicates per site (150 m^3 in total) were obtained using this active-sampling setup.

2.2. Contamination control

All steps realized followed extensive control measures to avoid cross contamination. First, all sampling materials were thoroughly cleaned prior to use, following established laboratory protocols. Filter holders, rings, stainless-steel filters, beakers and glass Petri dishes were heated to 420 °C to eliminate any residual organic matter or volatile compounds that could compromise analytical results and were covered with aluminium foil until subsequent uses and/or analysis. For its part, silicon 8 μm filters were not heat-treated for resistant reasons but were thoroughly cleaned in successive baths of absolute ethanol (99 %, Scharlau).

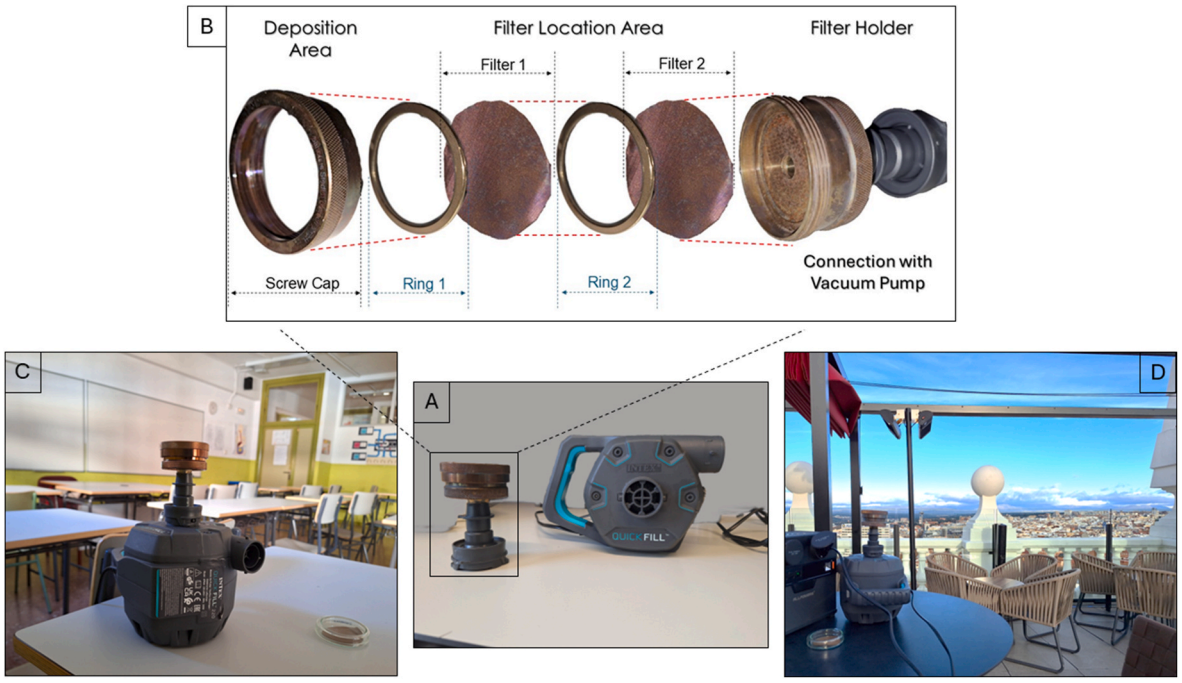

Fig. 1. Sampling devices used in this work. A. Pump and filter holder assembly. B. filter arrangement. C. Indoor sampling setup. D. Outdoor sampling setup.

Membranes were individually stored in pre-heated Petri dishes and examined under a stereomicroscope to confirm the absence of contamination before use.

For each individual sample, the filter holder previously mounted and heated was only opened for each use in order to keep it isolated. To complement and assess any potential background contamination, each sample included a dedicated control consisting of a Petri dish with a filter left open but not actively collecting air. This setup, previously validated in published studies, enabled quantification of ambient or handling-related contamination. Results are detailed in Supplementary Material (SM, Table S2)

Additional measures were implemented to minimize contamination from sampling personnel. In particular, as mentioned previously, the devices were consistently installed above ground level, with control in place to ensure that no individuals were in proximity during operation, as human presence could potentially bias the measurements. It was also controlled that the team wore exclusively bright coloured cotton garments to reduce the risk of introducing plastic microfibres and alert about cross contamination.

After confirming that microplastic counts on the control filters remained within acceptable thresholds, these values were subtracted from the corresponding sample data. Additional details on the experimental procedure can be found elsewhere (Gálvez-Blanca et al., 2024).

2.3. Analyses

Samples were transported to the laboratory and then, samples kept in Petri dishes were washed using cleaned beakers and ultrapure water. Preliminary tests using pilot samples led to the adoption of a three-step washing protocol with ultrapure water applied to both the rings and the filters. In those tests, this procedure was deemed sufficient to recover the majority of fibres, as stereomicroscopic examination confirmed the absence of residual fibres on the filters. However, formal validation of the method is still required with standardized fibres. The liquid was vacuum filtrated through 8 μm square silicone filters (Smart Membranes, MakroPor). Filters were subsequently stored in glass Petri dishes and dried at 60 °C for 24 h. Microparticles over these membranes were observed, classified and photographed using a Leica KL300 stereo microscope. The different typologies (fragment, fibre, film or filament) were selected following the criteria published elsewhere (Contreras et al., 2024). The images were analysed using the ImageJ software. Length, width, roundness and circularity parameters were used to discriminate between fragments and fibres as explained elsewhere (Rosal, 2021).

The identification of particles collected on the filters was performed using micro-Fourier Transform Infrared Spectroscopy (micro-FTIR). Analyses were conducted in two different laboratories using iN5 and iN10 microscopes (Thermo Scientific) respectively, both equipped with MCT detectors. To ensure the comparability of results between both instruments and sites, all measurements were carried out in transmission mode, under manual operation, and following identical experimental conditions: a spectral range of 4000-650 cm^{-1}, a resolution of 4 cm^{-1}, data spacing of 4 cm^{-1}, and 60 scans per sample. Polymer identification was achieved by comparing the obtained spectra with reference databases using OMNIC software, which applies Pearson correlation (Fig. S2). A Pearson match score $\geq$65 % was taken as a positive identification. This cut-off has already been adopted by other authors as a practical compromise that retains most true particles while keeping false positives to a minimum in natural samples (Botterell et al., 2022; Hildebrandt et al., 2024; K. Liu et al., 2019).

To guarantee strict comparability, the same μ-FTIR settings were applied to a broad panel of reference textiles, including plastic and animal origin polymers (acrylic, polyester, nylon and wool) but mainly cellulose-based fibres (cotton, linen, viscose, modal, Tencel) complemented by a set of plant-derived individuals. Those materials included differences in colour and ageing. For this purpose, materials were also exposed to environmental degradation during 1 and 3 months, and their respectively spectra were collected. With this, library spectra and real-sample spectra shared identical acquisition conditions (Table S3 and SM)

Additionally, to capture finer bulk features that are not resolved in the microscopic mode, each reference material explained before was then examined by ATR-FTIR. Five spectra were collected per material using a Nicolet iS20 FTIR spectrometer (Thermo Scientific) in transmittance mode with 60 scans and 4 cm^{-1} spectral resolution.

2.4. Calculations

Particle concentrations were derived in three steps. First, every particle visible on the entire filter was counted under the microscope to obtain the total item load. Second, a statistically representative FTIR subsample was analysed to determine what share of those items were plastic versus cellulosic; the subsample size was set to keep the identification error for any polymer class below 10 %, meeting the accuracy benchmark of (Cowger et al., 2024). Finally, the item counts for each fibre type were normalised to the total volume of air that passed through the sampler, yielding concentrations expressed as items per cubic metre.

Secondly, mass concentration was estimated for fibres by assuming a cylindrical shape and using the tabulated average density of each polymer, as shown in Table S4 (SM). For films and fragments, which were found in much lower amounts, volume was approximated as an ellipsoid, with the third unmeasured dimension taken as the average of the other two. Additional details on the estimation of particle mass from two-dimensional images are available elsewhere (Contreras et al., 2024; Rosal, 2021).

2.5. Chemometric procedure

Infrared spectra from the particles of interest were processed using Sartorius' SIMCA® 18 software for multivariate data analysis. This software tool has been specifically designed to perform multivariate analysis, including data exploration and group discrimination. To perform those discriminant analysis, each particle evaluated was carefully defined, and a complete matrix was generated, incorporating all relevant information. This included a total of 7 qualitative variables (environment, material, origin, colour, ageing status, replica, identification group) and the 6949 points included in the wavelength as quantitative variables.

2.5.1. Identification of key regions on infrared spectra

In this section, spectra obtained with ATR-FTIR was subjected to chemometric analysis. Prior to modelling, all spectra were pre-processed to ensure comparability. The pre-processing steps included standardization using the standard normal variate method, baseline correction with the asymmetric least squares method, and smoothing with the Savitzky-Golay method (7 points). The organisation of work, as shown in Scheme 1, consisted first of an analysis of standard materials with Orthogonal Partial Least Squares Discriminant Analysis (OPLS-DA) to identify and interpret key spectral regions.

Once discriminant analysis separate groups, those are faced by performing group-to-group comparisons. This software assigned scores to different wavelength peaks, highlighting the contribution of each spectral region. The peaks corresponding to these scores were evaluated and quantified to determine which spectral regions were most significant in distinguishing between the various materials.

2.5.2. Reclassification of doubtful cellulosic samples

As detailed in Section 2.3, spectra obtained with micro-FTIR, from all sampling sites were first compared with the reference libraries and identified using Pearson correlation (match >65 %). Later, each particle was then classified in one of three confidence tiers: good (>65 % match), doubtful (50–65 %), or no evidence (<50 %). Our subsequent discriminant analysis focuses on the doubtful and no-evidence groups, exploring whether multivariate chemometrics can retrieve discriminating information that simple pairwise matching overlooks. In addition, any spectrum from good match whose two best library hits differed by fewer than five correlation points, indicating near-degenerate similarity, was re-examined with the same chemometric workflow to resolve possible misclassifications.

For every environmental particle the workflow proceeded as follows.

1. The particle of interest spectrum was appended to the reference matrix and an individual OPLS-DA model was recalculated in SIMCA 18.
2. The Hotelling T^2 statistic, a multivariate distance to the model centroid, was obtained for the particle and for each reference spectrum.
3. Within every reference class the T^2 values were standardised ($T^{2*} = [T^2 - \mu]/\sigma$), thereby expressing distances as z-scores that account for intra-class variability.
4. The particle was first assigned to the broader category natural vs. industrial according to the class delivering the lowest normalised distance, and then to the specific fibre type that showed the minimum z-score.

2.5.3. OPLS-DA model validation

The quality and robustness of the models generated was assessed through a structured validation approach. The OPLS-DA models were built upon a fixed library of 42 reference spectra including 37 industrial-textile samples (spanning diverse dyes and artificial-ageing stages) and 5 unprocessed plant-derived fibres at the natural end of the cellulose spectrum.

To classify environmental fibres, each unknown spectrum was projected onto the same reference ser after recalibrating the OPLS-DA model. Then classification was determined by its Hotelling's T^2 distance. By using this methodology, it is ensured that every spectrum was treated as an external validation.

Further evaluation of the model performance was conducted using

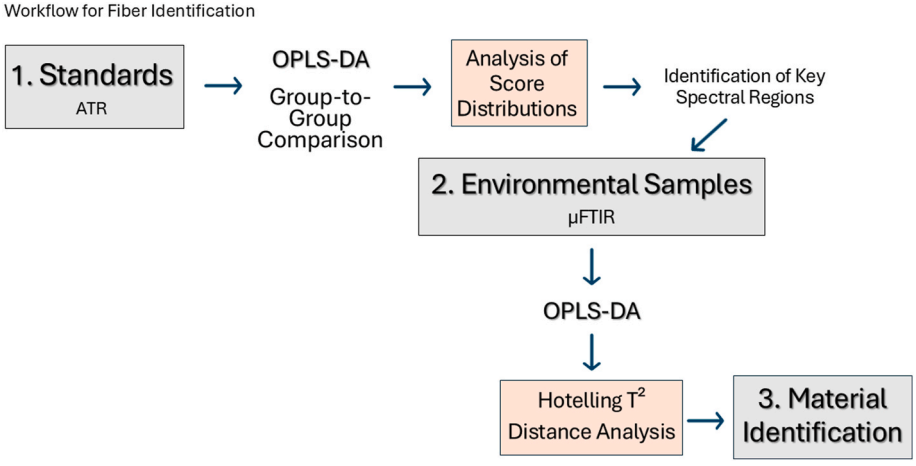

Scheme 1. Workflow for the chemometric procedure used in fibre identification.

multiple metrics: cumulative explained variance in the spectral (R^2X (cum)) and class (R^2Y(cum)) domains; cross-validated predictive ability (Q^2(cum)) and the R^2Y-Q^2 gap as an overfitting indicator. Additionally, significance testing was performed through Cross Validation ANOVA (CV-ANOVA) with a p-value threshold of <0.01, alongside permutation-test intercepts for R^2Y and Q^2.

To detect potential outlier, hypothesis testing was carried out using Hotelling's T^2 test (Bylesjö et al., 2006). Representative examples of this validation procedure for selected items are shown in Table S5.

3. Results and discussion

3.1. Abundances in number and mass concentrations

The morphological analysis of our samples revealed that fibres overwhelmingly dominated across other shapes in all locations and environments, accounting for 96 % of the observed particles of potential anthropogenic origin. This prevalence aligns with the fact that fibres, whether flat or round, can undergo long-range atmospheric transport (Xiao et al., 2023). Regarding the double filter technique used, data showed that most of particles were retained in the external filters (averaging 87 %). Furthermore, in all the tests performed, at least one particle appeared in the internal filter highlighting the importance of the double filter system to avoid underestimations. A schematic representation of the retention in the external filter is showed in Fig. S3. It was observed that particles were mainly retained in the central part of the filter.

For its part, films and fragments, which comprised the remaining 4 %, were detected only sporadically in both indoor and outdoor environments, and their identification was not controversial. Therefore, the chemometric study described below was restricted to fibres.

A total of 432 fibres were detected in Madrid, 240 in Tarragona (Vila-Seca and Ebro Delta), 158 in Gran Canaria, and 218 in Tenerife. In Madrid, indoor and outdoor counts were similar, although slightly higher outdoors. In Tarragona-Ebro Delta we found the higher average concentration (0.90 fibres/m^3). In Tenerife, fibre counts reached 0.24 fibres/m^3 (indoor) and 0.12 fibres/m^3 (outdoors), while for Gran Canaria, the same figures were 0.80 fibres/m^3 (indoor) and 0.26 fibres/m^3 (outdoor).

Infrared analysis of the sampled particles revealed a low diversity of materials. Cellulose was predominant, accounting for over 90 % of the tested particles, all of them in fibre form. Concerning MPs, the polymers found were polyethylene (PE), acrylic polymers (ACR), polypropylene (PP) and polyester (PES) in that order, for outdoor samples, and while PES represented >90 % of the MPs in indoor environments (Fig. S4 and SM). This observation aligns with findings from other studies, where polyester fibres have been reported to represent up to 94 % of indoor microplastics (Vianello et al., 2019). Nevertheless, indoor environments often show considerable variability, making direct comparisons between studies challenging (O'Brien et al., 2023). The concentration of MPs ranged from 0 to 0.04 MP/m^3, with the lowest value recorded in the natural zone of the Ebro Delta and the highest in outdoor samples from Madrid. On average, MP concentrations were similar between outdoor and indoor environments. Concerning cellulose fibres (CFs), the concentrations were typically one order of magnitude higher, ranging from 0.09 to 0.91 CFs/m^3. Similar to MPs, the average CF concentrations were comparable between indoor and outdoor samples (Fig. 2).

Fibre size displayed significant differences between indoor and outdoor samples. The equivalent diameter of fibres in indoor environments ranged from 13.8 to 398.4 μm, with an average of 84.4 ± 47.5 μm compared to 20.1–593.1 μm and an average of 116.4 ± 78.1 μm from outdoor fibres (Fig. S5 and SM). Due to the broad size distribution these differences were not statistically significant (*p*-value 0.198, Mann−Whitney *U* test). It is interesting to note that, although fibres captured in external filters were significantly longer (353 μm) than those in internal filters (319 μm) with a *p*-value of 0.002 in the Mann-Whitney *U* test, the data still showed that some long fibres passed through to the internal filter.

An important factor that determines the environmental fate of airborne particles is the aerodynamic diameter, that is defined as that of the sphere with unit (or reference) density settling with the same velocity as the particle. For the case of fibres, the aerodynamic diameter is closely related to the physical diameter (Rosal, 2021). Our results showed that the physical diameters of fibres sampled in indoor environments, average 28.3 μm (8.6–89.3 μm range) was significatively (*p*-value <0.01), Mann−Whitney *U* test) smaller than those from outdoor samples, average 42.0 μm (9.1–318 μm range). The smaller size of indoor fibres is associated with longer suspension times and a potentially increased risk of inhalation in indoor environments (J. Liu et al., 2022). The sizes described here are clearly compatible with the presence of these fibres in PM_{10} analyses, although they are slightly larger than those in $PM_{2.5}$, where they would only be present in a degraded

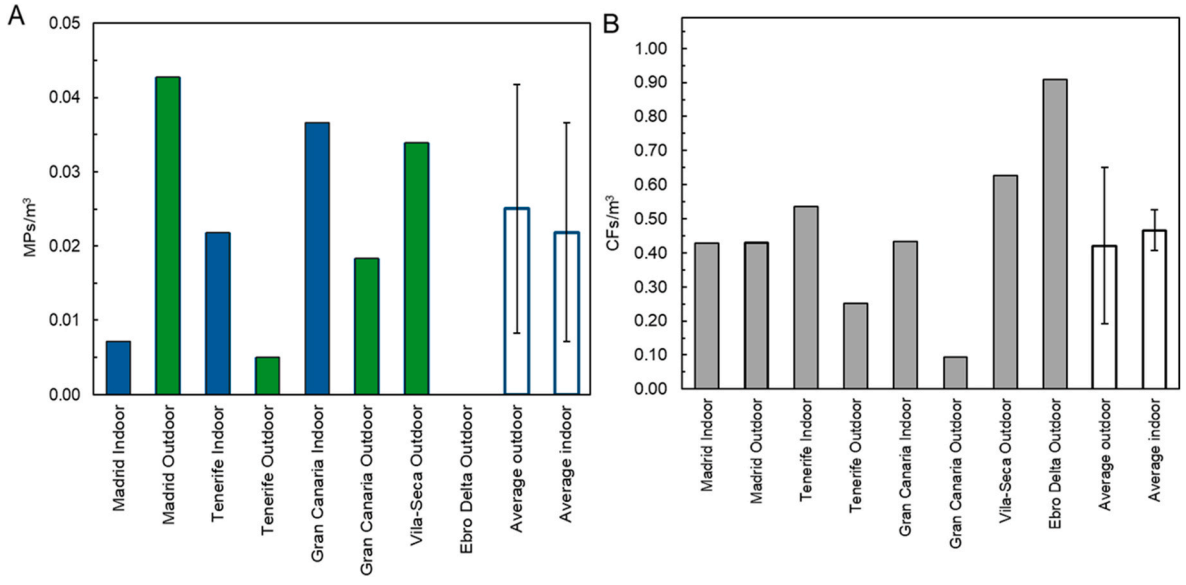

Fig. 2. Concentrations of MPs (A) and cellulose fibres (CFs) measured in indoor and outdoor environments. Environment-specific average values are included for reference with their corresponding standard deviation.

condition. According to the average figures estimated by the European Environment Agency in its 2024 report, these materials could be contributing to PM_{10} levels that are currently exceeding the recommended 50 μg/m^3 threshold in various locations, including those sampled (European Environment Agency, 2024) and that can be consulted in the supplementary material (SM, Table S6). This evidence also underscores the significance of fibre size in assessing environmental exposure and potential health impacts.

Based on the geometric characterization of the particles and their corresponding densities, we estimated an average mass concentration of MPs of 19 ng/m^3 in outdoor samples and 8.3 ng/m^3 in indoor samples, which primarily consisted of fibres, as previously noted. The mass concentrations of CFs were 197 ng/m^3 and 149 ng/m^3 in indoor and outdoor environments, respectively. Interestingly, although the number concentrations were similar in indoor and outdoor samples (as shown in Fig. 2), mass concentrations were considerably higher outdoors due to the larger size of fibres recovered from those samples. Converting particle numbers into mass can be controversial. Techniques such as pyrolysis-gas chromatography-mass spectrometry have been used for this purpose but pose significant challenges, as recently discussed (Rauert et al., 2025). Alternatively, geometric calculations have proven capable of providing accurate estimates of plastic particle mass concentrations from two-dimensional images. Although individual deviations may occur, they often cancel each other out, resulting in total errors below 5 %, particularly in samples with a low proportion of platelike particles, where the loss of thickness information can otherwise lead to larger inaccuracies (Barchiesi et al., 2023; Contreras et al., 2024). To the best of our knowledge, this is the first time the mass concentration of airborne MPs and CFs has been reported in atmospheric samples using geometric calculations.

Fibre colour can offer valuable insights into their potential origins. Bright and distinctive colours, such as blue, red, or pink, are rare in natural environments, making them reliable indicators of artificial sources, as demonstrated in previous studies (Finnegan et al., 2022; Gálvez-Blanca et al., 2024). In this study, over 70 %, and in some cases up to 90 %, of the fibres in both indoor and outdoor samples across all locations were transparent or white (Table S7 and SM).

The predominance of clear fibres aligns with findings in the literature, which report a significant presence of transparent or white fibres in various environments, sometimes attributed to bleaching processes during pretreatment (Zhang et al., 2020). The prevalence of clear-coloured fibres complicates their traceability, making it challenging to distinguish between artificial and natural origins. Generally, fibres with obvious non-natural colours can be associated with human-made sources. However, assuming that clear fibres are primarily of natural origin may underestimate their potential risks, as chemical oxidation, UV exposure, and other processes can alter fibre colour, potentially increasing the proportion of uncoloured fibres (H. Luo et al., 2020).

Tables S8 and S9 (see SM) present the results of a selection of recent studies focused on the presence of MPs in outdoor and indoor air in which the presence of cellulose is occasionally acknowledged. For reasons of consistency, the selection is limited to studies that used spectroscopic techniques, specifically micro-FTIR or micro-Raman, for characterization. In general, studies that do not employ spectroscopic characterization tend to report higher concentration values, reaching hundreds of MPs/m^3 (Liao et al., 2021; Sarathana and Winijkul, 2023; Zhu et al., 2021). The data reported in the literature indicates higher concentrations in indoor environments compared to outdoor environments, with values typically ranging from zero to a few units per cubic meter, except for some outliers. The observed variability may be attributed to local factors and the use of subsamples, which are sometimes very small and contain only a few occurrences, limiting the representativeness of the resulting statistical parameters (Abbasi et al., 2023; Dris et al., 2017). A source of variability, which might explain the observed variability, is the volume of air filtered as higher abundances and greater variation coefficients are associated to sampling volumes below 5 m^3 (K. Liu et al., 2019). As shown in Tables S8 and S9, most results indicate a high proportion of fibres, sometimes accounting for the entire set of anthropogenic particles reported. While many studies overlooked natural and CFs, in cases where they were included, cellulose and semi-synthetic cellulose made up as much as two-thirds of the total particle count. Similar to it, our results concluded that cellulose in samples is at least 10 times more abundant than MPs.

3.2. Chemometric study of cellulose materials

In this study, we used mid-infrared spectroscopy to determine the nature of CFs, which can originate from either natural or anthropogenic sources. First, we used ATR-FTIR to analyse standard materials, as it is a robust technique employed in most databases for identification purposes. The chemometric analysis started by data screening using principal component analysis (PCA) using the whole infrared spectra. This demonstrated that natural plants (e.g., hair-like structures on leaves or stems) exhibited distinctive characteristics compared to the anthropogenic fibres (Fig. S6 and SM). As shown in Fig. S7 (SM), cotton and linen fabrics formed a cluster due to their comparable characteristics based on infrared spectra, closely aligning with paper and cellulose. However, the manufactured materials viscose, Tencel, and modal formed separate clusters. Specifically, viscose and Tencel exhibited close similarities to one another, while modal was closer to them than to cotton and linen (Figs. S7 and S8, SM).

To gain a better understanding of the differences between remains from natural plants and textiles using mid-infrared data, a discriminant analysis was performed, revealing specific structural patterns. Contribution plots from the OPLS-DA analysis, comparing the two groups, were examined to identify the variables responsible for their differentiation. These plots highlight key variables that fall outside the 3 standard deviation range, ensuring a robust analysis. The chemometric analysis identified three key spectral regions consistently highlighted across all analyses: 3700-3100 cm^{-1}, 3010-2800 cm^{-1}, and the 1850-650 cm^{-1} range, commonly identified as fingerprint region. The differences between plant-derived fibres and textile-based cellulose were revealed primarily attributed to a reduced set of functional groups as shown in Fig. 3A. Textile fibres (e.g., textile cotton) displayed characteristic cellulose absorption bands (3760-3460 cm^{-1} and 3280 cm^{-1} corresponding to hydroxyl groups and 1290-760 cm^{-1} for C-O bonds), whereas natural plant fibres presented additional signatures corresponding to hemicellulose and lignin (3210-2490 cm^{-1} for carboxylic/hydroxyl groups and 1690-1300 cm^{-1} for C=O and C=C bonds (Chung et al., 2004; Yang et al., 2007). Further differences emerged between textile cotton and chemically modified cellulose (e.g., viscose) as shown in Fig. 3B. Cotton natural cellulose exhibited O-H stretching (3560-3460 cm^{-1}), C-H vibrations from glycosidic structures (~2890 cm^{-1}), and distinct C-O/C-O-C signals (~1070 and 1020 cm^{-1}) (X. Liu et al., 2021), whereas viscose showed broader O-H stretching features with reduced crystallinity (3795-3575 cm^{-1}) (Lin-Vien et al., 1991), carbonyl groups (~1730 cm^{-1}, and esterified or etherified C-O-C vibrations (1450, 1220-820 cm^{-1}) (Wu et al., 2014).

Finally, our analysis showed that it was possible to differentiate industrial CFs as shown in Fig. 4. Cotton fibres exhibited stronger O-H and C-H stretching linked to higher crystallinity, while modal, viscose, and Tencel showed broader O-H bands, carbonyl peaks, and altered C-O vibrations, indicating those arising from lower crystallinity and the chemical modifications introduced during regeneration (Carrillo et al., 2004).

3.3. Using Hotelling distance to characterize ambiguous spectra

The application of FTIR has demonstrated its capability to distinguish differences among different cellulose-based materials. However, conventional correlations (Pearson or Spearman) typically yield similar

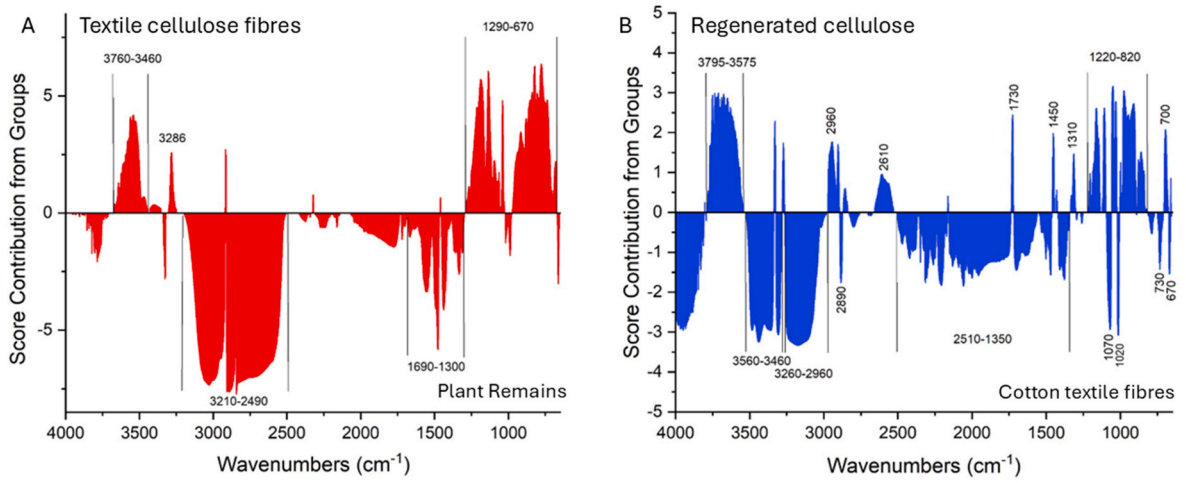

Fig. 3. Contribution scores comparing the spectral features of two groups: natural plant remains versus cellulose textiles (A), and cotton textiles versus regenerated celluloses (B).

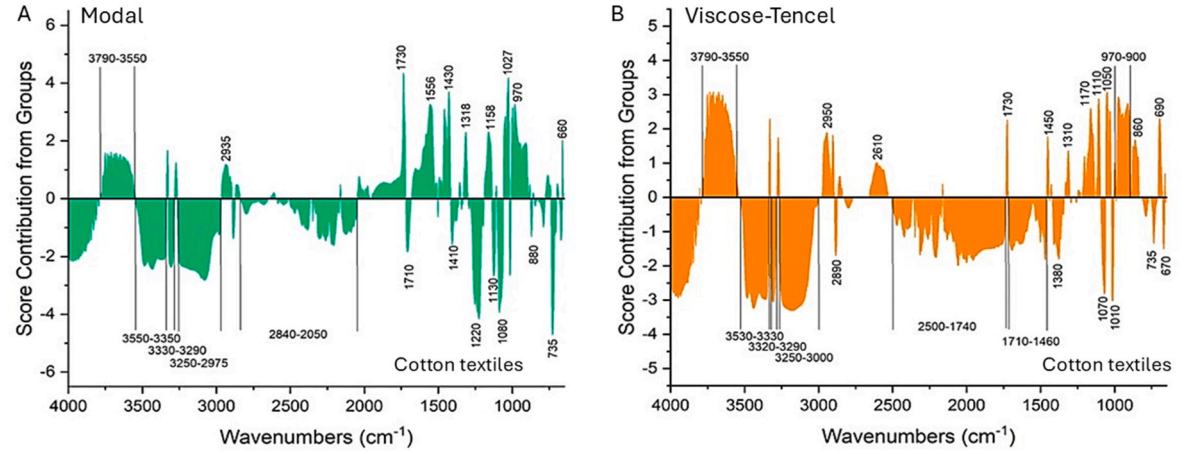

Fig. 4. Contribution scores comparing the spectral features cotton textiles versus modal (A), and cotton Textiles versus the regenerated cellulose fibres viscose and Tencel (B). The peaks displayed mark the wavelengths that best separate cotton from the fibre class under comparison in each case.

match percentages when applied to real world samples making it impossible to differentiate among the different cellulose-based materials. This is typical for very similar materials, as the mentioned correlations are inherently limited in capturing subtle differences among spectra. With this rationale, we performed a chemometric approach using discriminant analysis and Hotelling's T^2 distances to assess the differences among the spectra of CFs. This approach benefits from the structured use of all spectral information in discriminant analysis and Hotelling's distances enabling a more comprehensive evaluation of differences between materials even outside from normality (Kariya, 1981). By considering both variance and covariance within the data Hotelling's distances provide a robust metric for distinguishing between polymer types (Modarres, 2024). This method not only resolves ambiguities left by Pearson correlation but also ensures a more reliable and accurate differentiation of polymeric fibres in exercises of multiple variables and observations (IR spectrum peaks) (Haoran et al., 2020). The integration of statistical thresholds, such as Hotelling's T^2 critical values at the 95 % and 99 % confidence levels, improve classification accuracy by identifying samples that surpass these limits, while also uncovering subtle structural or compositional variations, providing a dependable framework for confidently identifying and categorizing complex materials.

For the application of Hotelling's T^2 tests, each particle spectrum was compared against a set of representative standard spectra for the materials under investigation. When performing OPLS-DA, the software identifies differences and classifies samples, accordingly, generating representative models within a multivariate framework. The clusters obtained can be visualized in Figures S6, S7 and S8 (Supplementary Material), which are different from PCA that simply explain data. In contrast, discriminant analysis, which uses statistical models to account for multidimensional variability, allowed particles to be accurately classified into specific categories. Hotelling's distances have been integrated into this process to further refine classification by quantifying the degree of similarity between individual particles and the standard materials. Specifically, this metric calculates how far an observation lies from the centre of the discriminant model (George et al., 2009), making it particularly effective for distinguishing materials with small spectral differences, such as cotton, Tencel, modal, and viscose. Hotelling's T^2 distances were calculated for the particle of interest and for various examples of each standard material in relation to the constructed model as shown in Fig. 5.

The distances for each material type were averaged (since multiple fabrics or tissues were evaluated using FTIR) and then compared with the particle of interest so that the most similar material could be identified. This process allows for improved matching that considers all the structural features in mid infrared spectra. Our results demonstrate that combining discriminant analysis with Hotelling's distances significantly enhanced the identification of cellulosic materials. This approach

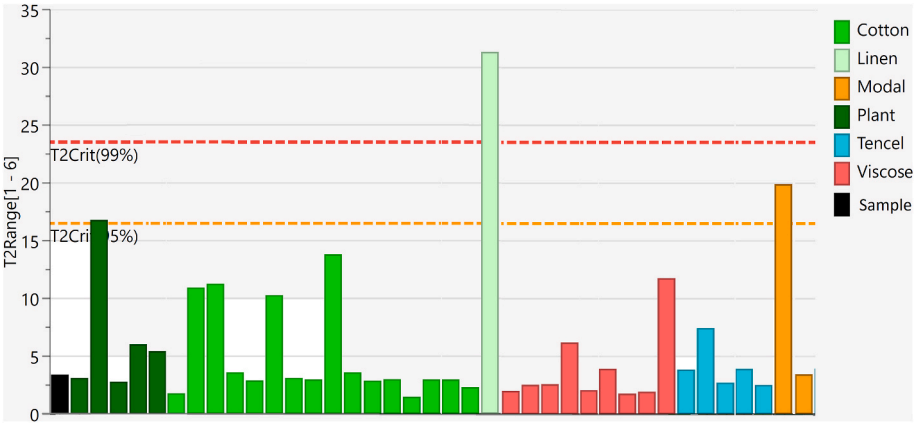

Fig. 5. Hotelling's T^2 Range plot for cellulose-based materials. The graph displays Hotelling's distances (T^2) for a given individual sample (in black) and standards coloured according to material type. Critical thresholds are also displayed.

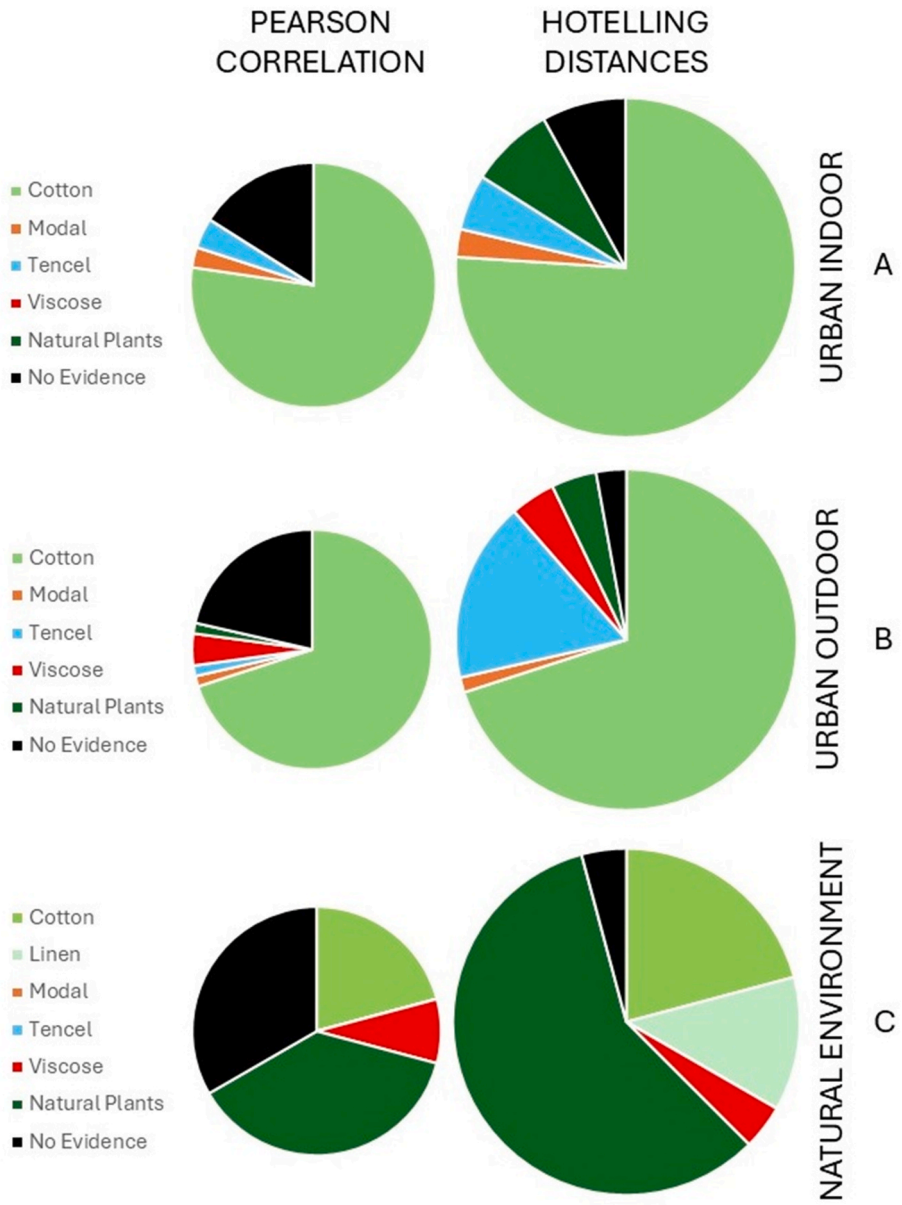

Fig. 6. Differences between Pearson correlation and assignments using Hotelling distances. Urban indoor (A), urban outdoor (B) and natural environment (C).

reduced the number of samples with insufficient evidence for clear classification, allowing for a more precise characterization of certain regenerated celluloses. The improvement is shown in Fig. 6, where the proportion of spectra classified as 'undefined' significantly dropped after applying Hotelling's analysis.

The improvement is clear in the Ebro Delta natural reserve for which inconclusive spectra (using Pearson correlation) dropped from 33 % to 4.2 % when most cellulose fibres could be identified as vegetal materials such as plant remains (Fig. 6C). In all samples, the method facilitated better identification of regenerated cellulose and enhanced the distinction between textile cotton and linen. After recalculating the undefined fraction of our samples, this study revealed that, in urban environments, regenerated cellulose accounted for 8 %–25 % of airborne CFs, depending on whether the samples were collected indoors or outdoors. Furthermore, more than 70 % of the identified celluloses, including cotton and linen, appeared to have undergone various treatments, with approximately 35 % of these materials being artificially modified or processed (modal, Tencel, and viscose). This suggests that processed textile products are also prevalent and actively circulate in the atmosphere.

The results of this study emphasize the importance of closely monitoring textiles and fabrics to assess exposure to anthropogenic fibres, a critical step for conducting risk assessments and mitigating their environmental and health impacts. While much attention has been focused on MPs, cellulose-derived materials, including regenerated cellulose, also raise concerns due to their processing methods and the additives used in their formulation. CFs, although derived from natural cellulose, undergo industrial processing that introduces additives and solvents with potential environmental and health consequences. These materials act not only as respirable particles but also as carriers of leachable chemicals, contributing to pollution and possible human exposure.

Although regenerated celluloses are derived from natural sources such as wood pulp, he chemical treatments it undergoes can make it a potential pollutant. Common textile additives include cationic softeners, reactive dyes, phosphorus-based flame retardants like TCPP, and biocides such as triclosan (Emam, 2019; Limpiteeprakan et al., 2016; Salmeia et al., 2016; Wedin et al., 2018). The production of viscose involves carbon disulfide (CS_2) and may release hydrogen sulphide (H_2S) (Robertson, 2000), which poses occupational health risks and has been linked to higher rates of chronic bronchitis among rayon workers compared to cotton-mill employees (Gondhalekar et al., 2022; Majumdar et al., 2022; Tan et al., 2002). Additionally, Tencel fibres are processed using N-methylmorpholine N-oxide, another chemical with potential environmental implications (Ciechańska et al., 2009).

Residual compounds from these processes can leach into water systems through washing and degradation, impacting aquatic ecosystems and human health. Moreover, regenerated cellulose fibres can remain airborne, raising concerns about inhalation exposure. Studies indicate that cellulose nano- and micro-fibres (0.1–5 μm in diameter) provoke persistent granulomatous inflammation in rat lungs, highlighting a combined physical and chemical hazard (Fujita et al., 2021). Like MPs, CFs can reach respiratory tissues, trigger inflammation, and transport contaminants or microorganisms (Baeza-Martínez et al., 2022). Therefore, it is needed to assess both fibre load and additive release potential to fully understand the environmental and health risks of these compounds.

3.4. Future prospective

An obvious next step is to extend the atmospheric picture with cross-matrix sampling. Quantifying the same fibre classes in local soils, surface waters and bed sediments would allow mass-balance estimates and reveal whether the air compartment is a transient sink or a major redistribution pathway. Parallel datasets could also clarify whether periods of high atmospheric loading translate into measurable deposition pulses on land or in receiving waters. Equally important is the standardisation of cellulosic and mixed-composition microfibres. At present, no certified reference materials in micro and nano size exist for this typology, hampering interlaboratory comparisons and biasing calibration curves towards synthetic polymers. Developing well-characterised Standard Reference Materials (SRM), covering pristine, dyed and weathered states would normalise extraction yields. Finally, this chemometric workflow should be stress-tested against spectra obtained with emerging high-throughput platforms such as LDIR, FPA-μ-FTIR and O-PTIR. Benchmarking the model performance across these technologies will indicate how transferable the discriminant rules are and whether instrument-specific retraining is required before routine implementation.

4. Conclusions

Our data show that cellulose-based fibres, not plastic fragments, constitute the bulk of the respirable aerosol. Indoors they contribute an order of magnitude more mass than conventional microplastics (179 ng/m^3 vs 14 ng/m^3), indicating that current PM metrics and MPs inventories systematically undervalue a major anthropogenic contaminant.

Indoor fibres are markedly thinner, remain airborne longer, and therefore have a higher probability of reaching the deep lung. This finding highlights the need to assess domestic and occupational exposure to cellulosic fibres alongside the better-studied plastic particles.

Coupling transmission μ-FTIR with OPLS-DA and Hotelling distances reduced the "ambiguous" category by ~40 % compared with direct spectral matching, and successfully distinguished cotton/linen from regenerated cellulose (viscose, Tencel, modal) without relying on dyes or chemical markers.

The results underscore the urgency of developing certified reference materials specifically for cellulosic microfibres and of expanding industrial spectral libraries; without these tools, inter-laboratory comparability will remain limited.

By revealing that a substantial share of the "invisible" fibre load originates from textiles rather than natural sources, our study paves the way for including "anthropogenic cellulosic fibres" as a distinct category in air-quality surveillance and health-impact evaluations.

CRediT authorship contribution statement

Carlos Edo: Writing – review & editing, Writing – original draft, Visualization, Supervision, Software, Project administration, Methodology, Investigation, Formal analysis, Conceptualization. **Marica Erminia Schiano:** Writing – review & editing, Writing – original draft, Methodology, Investigation, Formal analysis, Conceptualization. **Sergio J. Álvarez-Méndez:** Writing – original draft, Methodology, Investigation, Formal analysis. **Javier Hernández-Borges:** Writing – original draft, Visualization, Supervision, Resources, Investigation, Formal analysis. **Daura Vega-Moreno:** Writing – original draft, Methodology, Formal analysis. **Ana Molina-Rodríguez:** Investigation. **May Gómez:** Writing – original draft, Methodology, Conceptualization. **Alicia Herrera:** Writing – original draft, Methodology, Investigation. **Miguel González-Pleiter:** Writing – original draft, Supervision, Methodology, Funding acquisition, Conceptualization. **Francisca Fernández-Piñas:** Writing – original draft, Supervision, Resources, Project administration, Methodology, Funding acquisition. **Roberto Rosal:** Writing – original draft, Visualization, Validation, Resources, Project administration, Methodology, Funding acquisition, Data curation, Conceptualization.

Declaration of competing interest

The authors declare that they have no known competing financial interests or personal relationships that could have appeared to influence the work reported in this paper.

Acknowledgments

Authors acknowledge the financial support provided by Plastics Europe and the Spanish Government, (Ministry of Science, grants PID2020-113769RB-C21/C22 and PID2023-146111OB-I00). The authors would also like to thank RIU Hotels & Resorts, CEPA José Luis Sampedro, and IES Alkal'a Nahar for generously providing their facilities for sample collection, as well as the Environmental Unit of the Port Authority of Las Palmas (APLP) for their collaboration in sample collection.

Appendix A. Supplementary data

Supplementary data to this article can be found online at https://doi.org/10.1016/j.envres.2025.122082.

Abbreviations

MP, MP(s)	Microplastics.
CF, CFs	Cellulose Fibres.
ACR	Acrylic Polymers
PP	Polypropylene
PE	Polyethylene
PES	Polyester

Data availability

Data will be made available on request.

References

Abbasi, Sajjad, Jaafarzadeh, Neamatollah, Zahedi, Amir, Ravanbakhsh, Maryam, Abbaszadeh, Somayeh, Turner, Andrew, 2023. Microplastics in the atmosphere of Ahvaz City, Iran. J. Environ. Sci. 126, 95–102. https://doi.org/10.1016/j.jes.2022.02.044.

Ageel, Hassan Khalid, Harrad, Stuart, Abdallah, Mohamed Abou-Elwafa, 2024. Microplastics in indoor air from Birmingham, UK: implications for inhalation exposure. Environ. Pollut. 362, 124960. https://doi.org/10.1016/j.envpol.2024.124960.

Amato-Lourenço, Luís Fernando, Bertoldi, Crislaine, van Praagh, Martijn, Rillig, Matthias, 2025. Environmental factors influence airborne microplastic deposition in the soil of urban allotment gardens. Environ. Pollut. 375, 126372. https://doi.org/10.1016/j.envpol.2025.126372.

Azari, Aala, Ronsmans, Steven, Vanoirbeek, Jeroen A.J., Hoet, Peter H.M., Ghosh, Manosij, 2024. Challenges in Raman spectroscopy of (micro)Plastics: the interfering role of colourants. Environ. Pollut. 363, 125250. https://doi.org/10.1016/j.envpol.2024.125250.

Baeza-Martínez, Carlos, Olmos, Sonia, González-Pleiter, Miguel, López-Castellanos, Joaquín, García-Pachón, Eduardo, Masiá-Canuto, Mar, Bayo, Javier, 2022. First evidence of microplastics isolated in European citizens' lower airway. J. Hazard Mater. 438, 129439. https://doi.org/10.1016/j.jhazmat.2022.129439.

Barchiesi, Margherita, Kooi, Merel, Koelmans, Albert A., 2023. Adding depth to microplastics. Environ. Sci. Technol. 57 (37), 14015–14023. https://doi.org/10.1021/acs.est.3c03620.

Botterell, Zara L.R., Bergmann, Melanie, Hildebrandt, Nicole, Krumpen, Thomas, Steinke, Michael, Thompson, Richard C., Lindeque, Penelope K., 2022. Microplastic ingestion in zooplankton from the Fram Strait in the Arctic. Sci. Total Environ. 831, 154886. https://doi.org/10.1016/j.scitotenv.2022.154886.

Bylesjö, Max, Rantalainen, Mattias, Cloarec, Olivier, Nicholson, Jeremy K., Holmes, Elaine, Trygg, Johan, 2006. OPLS discriminant analysis: combining the strengths of PLS-DA and SIMCA classification. J. Chemometr. 20 (8-10), 341–351.

Carrillo, F., Colom, X., Suñol, J.J., Saurina, J., 2004. Structural FTIR analysis and thermal characterisation of lyocell and viscose-type fibres. Eur. Polym. J. 40 (9), 2229–2234. https://doi.org/10.1016/j.eurpolymj.2004.05.003.

Chung, Chinkap, Lee, Myunghee, Choe, Eun Kyung, 2004. Characterization of cotton fabric scouring by FT-IR ATR spectroscopy. Carbohydr. Polym. 58 (4), 417–420. https://doi.org/10.1016/j.carbpol.2004.08.005.

Ciechańska, D., Wesołowska, E., Wawro, D., 2009. An introduction to cellulosic fibres. In: Eichhorn, S.J., Hearle, J.W.S., Jaffe, M., Kikutani, T. (Eds.), Handbook of Textile Fibre Structure. Woodhead Publishing, pp. 3–61.

Contreras, Laura, Edo, Carlos, Rosal, Roberto, 2024. Mass concentration of plastic particles from two-dimensional images. Sci. Total Environ. 946, 173849. https://doi.org/10.1016/j.scitotenv.2024.173849.

Cottom, Joshua W., Cook, Ed, Velis, Costas A., 2024. A local-to-global emissions inventory of macroplastic pollution. Nature 633 (8028), 101–108. https://doi.org/10.1038/s41586-024-07758-6.

Cowger, W., Markley, L.A.T., Moore, S., Gray, A.B., Upadhyay, K., Koelmans, A.A., 2024. How many microplastics do you need to (sub)sample? Ecotoxicol. Environ. Saf. 275, 116243. https://doi.org/10.1016/j.ecoenv.2024.116243.

Darbra, R.M., González-Dan, J.R., Casal, J., Àgueda, A., Capri, E., Fait, G., Guillén, D., 2012. Additives in the textile industry. In: Barceló, D., Kostianoy, A.G. (Eds.), Global Risk-based Management of Chemical Additives I: Production, Usage Amd Environmental Occurrence, vol. 18. Springer, pp. 83–107.

Dehaut, Alexandre, Hermabessiere, Ludovic, Duflos, Guillaume, 2022. Microplastics detection using Pyrolysis-GC/MS-Based methods. In: Rocha-Santos, Teresa, Costa, Monica F., Mouneyrac, Catherine (Eds.), Handbook of Microplastics in the Environment. Springer International Publishing, Cham, pp. 141–175.

Dris, Rachid, Gasperi, Johnny, Mirande, Cécile, Mandin, Corinne, Guerrouache, Mohamed, Langlois, Valérie, Tassin, Bruno, 2017. A first overview of textile fibers, including microplastics, in indoor and outdoor environments. Environ. Pollut. 221, 453–458. https://doi.org/10.1016/j.envpol.2016.12.013.

Edo, Carlos, Fernández-Piñas, Francisca, Leganes, Francisco, Gómez, May, Martínez, Ico, Herrera, Alicia, González-Pleiter, Miguel, 2023. A nationwide monitoring of atmospheric microplastic deposition. Sci. Total Environ. 905, 166923. https://doi.org/10.1016/j.scitotenv.2023.166923.

Emam, Hossam E., 2019. Antimicrobial cellulosic textiles based on organic compounds. 3 Biotech 9 (1), 29. https://doi.org/10.1007/s13205-018-1562-y.

European Environment Agency, 2022. Microplastics from Textiles: towards a Circular Economy for Textiles in Europe. Retrieved from Copenhagen, Denmark.

European Environment Agency, 2024. Europe'S Air Quality Status 2024. https://doi.org/10.2800/5970. Briefing no. 06/2024.

Finnegan, Alexander Matthew David, Süsserott, Rebekah, Gabbott, Sarah E., Gouramanis, Chris, 2022. Man-made natural and regenerated cellulosic fibres greatly outnumber microplastic fibres in the atmosphere. Environ. Pollut. 310, 119808. https://doi.org/10.1016/j.envpol.2022.119808.

Fujita, Katsuhide, Obara, Sawae, Maru, Junko, Endoh, Shigehisa, 2021. Pulmonary inflammation following intratracheal instillation of cellulose nanofibrils in rats: comparison with multi-walled carbon nanotubes. Cellulose (Lond.) 28 (11), 7143–7164. https://doi.org/10.1007/s10570-021-03943-2.

Gálvez-Blanca, Virginia, Edo, Carlos, González-Pleiter, Miguel, Fernández-Piñas, Francisca, Leganés, Francisco, Rosal, Roberto, 2024. Microplastics and non-natural cellulosic particles in Spanish bottled drinking water. Sci. Rep. 14 (1), 11089. https://doi.org/10.1038/s41598-024-62075-2.

George, Joval P., Chen, Zheng, Shaw, Philip, 2009. Fault detection of drinking water treatment process using PCA and Hotelling's T2 chart. Int. J. Comput. Inform. Eng. 3 (2), 430–435.

Gondhalekar, Sachin C., Pawar, Pravin J., Dhumal, Sunil S., Thakre, Shirish, 2022. Fate of CS2 in viscose process: a chemistry perspective. Cellulose (Lond.) 29 (3), 1451–1461. https://doi.org/10.1007/s10570-021-04398-1.

González-Pleiter, Miguel, Edo, Carlos, Aguilera, Ángeles, Viúdez-Moreiras, Daniel, Pulido-Reyes, Gerardo, González-Toril, Elena, Rosal, Roberto, 2021. Occurrence and transport of microplastics sampled within and above the planetary boundary layer. Sci. Total Environ. 761, 143213. https://doi.org/10.1016/j.scitotenv.2020.143213.

Gündoğdu, Sedat, Bour, Agathe, Köşker, Ali Rıza, Walther, Bruno Andreas, Napierska, Dorota, Florin-Constantin, Mihai, Walker, Tony R., 2024. Review of microplastics and chemical risk posed by plastic packaging on the marine environment to inform the Global Plastics Treaty. Sci. Total Environ. 946, 174000. https://doi.org/10.1016/j.scitotenv.2024.174000.

Haoran, L., Alexander, A., Debashis, P., Jie, P., Pei, W., 2020. An adaptable generalization of Hotelling's T^2 test in high dimension. Ann. Stat. 48, 1815–1847.

Hildebrandt, L., Fischer, M., Klein, O., Zimmermann, T., Fensky, F., Siems, A., Pröfrock, D., 2024. An analytical strategy for challenging members of the microplastic family: particles from anti-corrosion coatings. J. Hazard Mater. 470, 134173. https://doi.org/10.1016/j.jhazmat.2024.134173.

Käppler, Andrea, Fischer, Marten, Scholz-Böttcher, Barbara, M., Oberbeckmann, Sonja, Labrenz, Matthias, Fischer, Dieter, Voit, Brigitte, 2018. Comparison of μ-ATR-FTIR spectroscopy and py-GCMS as identification tools for microplastic particles and fibers isolated from river sediments. Anal. Bioanal. Chem. 410 (21), 5313–5327. https://doi.org/10.1007/s00216-018-1185-5.

Kariya, Takeaki, 1981. A robustness property of Hotelling's T^2-test. Ann. Stat. 211–214.

Liao, Zhonglu, Ji, Xiaoliang, Ma, Yuan, Lv, Baoqiang, Huang, Wei, Zhu, Xuan, Shang, Xu, 2021. Airborne microplastics in indoor and outdoor environments of a coastal city in Eastern China. J. Hazard Mater. 417, 126007. https://doi.org/10.1016/j.jhazmat.2021.126007.

Limpiteeprakan, Pawena, Babel, Sandhya, Lohwacharin, Jenyuk, Takizawa, Satoshi, 2016. Release of silver nanoparticles from fabrics during the course of sequential washing. Environ. Sci. Pollut. Control Ser. 23 (22), 22810–22818. https://doi.org/10.1007/s11356-016-7486-3.

Lin-Vien, D., Colthup, N.B., Fateley, W.G., Grasselli, J.G., 1991. Alcohols and phenols. In: Lin-Vien, D., Colthup, N.B., Fateley, W.G., Grasselli, J.G. (Eds.), The Handbook of Infrared and Raman Characteristic Frequencies of Organic Molecules. Academic Press, pp. 45–60.

Liu, Jianli, Liu, Qiang, An, Lihui, Wang, Ming, Yang, Qingbo, Zhu, Bo, Xu, Yuyao, 2022. Microfiber pollution in the Earth system. Rev. Environ. Contam. Toxicol. 260 (1), 13. https://doi.org/10.1007/s44169-022-00015-9.

Liu, Kai, Wang, Xiaohui, Wei, Nian, Song, Zhangyu, Li, Daoji, 2019. Accurate quantification and transport estimation of suspended atmospheric microplastics in megacities: implications for human health. Environ. Int. 132, 105127. https://doi.org/10.1016/j.envint.2019.105127.

Liu, Xuwei, Renard, Catherine M.G. C., Bureau, Sylvie, Le Bourvellec, Carine, 2021. Revisiting the contribution of ATR-FTIR spectroscopy to characterize plant cell wall

polysaccharides. Carbohydr. Polym. 262, 117935. https://doi.org/10.1016/j.carbpol.2021.117935.
Liu, Yuanli, Chand, Rupa, Dencker, Jytte, Hanning, Anne-Charlotte, Gunnerblad, Emma, Vollertsen, Jes, 2025. Are we overestimate the contribution of microplastics from industrial laundry? Microplastic exploration in an industrial laundry: quantification and elimination. J. Hazard Mater. 493, 138425. https://doi.org/10.1016/j.jhazmat.2025.138425.
López-Rosales, Adrián, Ferreiro, Borja, Andrade, Jose M., Kerstan, Andreas, Robey, Darren, Muniategui, Soledad, 2025. Reviewing the fundamentals and best practices to characterize microplastics using state–of–the-art quantum-cascade laser reflectance-absorbance spectroscopy. Trac. Trends Anal. Chem. 188, 118229. https://doi.org/10.1016/j.trac.2025.118229.
Luo, Dehua, Chu, Xinyun, Wu, Yue, Wang, Zhenfeng, Liao, Zhonglu, Ji, Xiaoliang, Shang, Xu, 2024. Micro- and nano-plastics in the atmosphere: a review of occurrence, properties and human health risks. J. Hazard Mater. 465, 133412. https://doi.org/10.1016/j.jhazmat.2023.133412.
Luo, Hongwei, Zhao, Yaoyao, Li, Yu, Xiang, Yahui, He, Dongqin, Pan, Xiangliang, 2020. Aging of microplastics affects their surface properties, thermal decomposition, additives leaching and interactions in simulated fluids. Sci. Total Environ. 714, 136862. https://doi.org/10.1016/j.scitotenv.2020.136862.
Majumdar, Deepanjan, Bhanarkar, Anil, Rao, Chalapati, Gouda, Dinabandhu, 2022. Carbon disulphide and hydrogen sulphide emissions from viscose fibre manufacturing industry: a case study in India. Atmos. Environ. X 13, 100157. https://doi.org/10.1016/j.aeaoa.2022.100157.
Miraftab, Mohsen, 2000. Technical fibres. In: R Horrocks, A., Anand, S.C. (Eds.), Handbook of Technical Textiles. CRC Press, Cambridge-England, pp. 24–41.
Modarres, Reza, 2024. Hotelling T^2 test in high dimensions with application to Wilks outlier method. Stat. Pap. 65 (8), 5203–5218.
Nacci, Tommaso, Sabatini, Francesca, Cirrincione, Claudia, Degano, Ilaria, Colombini, Maria Perla, 2022. Characterization of textile fibers by means of EGA-MS and Py-GC/MS. J. Anal. Appl. Pyrolysis 165, 105570. https://doi.org/10.1016/j.jaap.2022.105570.
Napper, I.E., Thompson, R.C., 2020. Plastic debris in the marine environment: history and future challenges. Glob Challenges 4 (6), 1900081. https://doi.org/10.1002/gch2.201900081.
O'Brien, Stacey, Rauert, Cassandra, Ribeiro, Francisca, Okoffo, Elvis D., Burrows, Stephen D., O'Brien, Jake W., Thomas, Kevin V., 2023. There's something in the air: a review of sources, prevalence and behaviour of microplastics in the atmosphere. Sci. Total Environ. 874, 162193. https://doi.org/10.1016/j.scitotenv.2023.162193.
Pagliaccia, Benedetta, Ascolese, Miriam, Vannini, Elena, Carretti, Emiliano, Lubello, Claudio, Gori, Riccardo, 2025. Methodologic insights aimed to set-up an innovative Laser Direct InfraRed (LDIR)-based method for the detection and characterization of microplastics in wastewaters. Sci. Total Environ. 967, 178817. https://doi.org/10.1016/j.scitotenv.2025.178817.
Parajuli, Prakash, Acharya, Sanjit, Rumi, Shaida Sultana, Hossain, Md Tanjim, Abidi, Noureddine, 2021. 4 - regenerated cellulose in textiles: rayon, lyocell, modal and other fibres. In: Mondal, Md Ibrahim H. (Ed.), Fundamentals of Natural Fibres and Textiles. Woodhead Publishing, pp. 87–110.
PlasticsEurope, 2023. Plastics—The Facts 2023. Retrieved from Brussels.
Rauert, Cassandra, Charlton, Nathan, Bagley, Angus, Dunlop, Sarah A., Symeonides, Christos, Thomas, Kevin V., 2025. Assessing the efficacy of pyrolysis–gas chromatography–mass spectrometry for nanoplastic and microplastic analysis in human blood. Environ. Sci. Technol. 59 (4), 1984–1994. https://doi.org/10.1021/acs.est.4c12599.
Robertson, R.C., 2000. Fibres - types. In: Siegel, Jay, Knupfer, Geoffrey, Saukko, Pekka (Eds.), Encyclopedia of Forensic Sciences, pp. 838–854. Roux, C.
Rosal, Roberto, 2021. Morphological description of microplastic particles for environmental fate studies. Mar. Pollut. Bull. 171, 112716. https://doi.org/10.1016/j.marpolbul.2021.112716.
Salmeia, Khalifah A., Gaan, Sabyasachi, Malucelli, Giulio, 2016. Recent advances for flame retardancy of textiles based on phosphorus chemistry, 8 (9), 319.
Sarathana, Danuwas, Winijkul, Ekbordin, 2023. Concentrations of airborne microplastics during the dry season at five locations in Bangkok metropolitan region, Thailand. Atmosphere 14 (1). https://doi.org/10.3390/atmos14010028.
Simon, Márta, van Alst, Nikki, Vollertsen, Jes, 2018. Quantification of microplastic mass and removal rates at wastewater treatment plants applying Focal Plane Array (FPA)-based Fourier Transform Infrared (FT-IR) imaging. Water Res. 142, 1–9. https://doi.org/10.1016/j.watres.2018.05.019.
Stanton, Thomas, Johnson, Matthew, Nathanail, Paul, MacNaughtan, William, Gomes, Rachel L., 2019. Freshwater and airborne textile fibre populations are dominated by 'natural', not microplastic, fibres. Sci. Total Environ. 666, 377–389. https://doi.org/10.1016/j.scitotenv.2019.02.278.
Tan, Xiaodong, Peng, Xiaoxia, Wang, Fuyuan, Joyeux, Michel, Hartemann, Philippe, 2002. Cardiovascular effects of carbon disulfide: meta-analysis of cohort studies. Int. J. Hyg Environ. Health 205 (6), 473–477. https://doi.org/10.1078/1438-4639-00174.
Tarafdar, Abhrajyoti, Xie, Junhao, Gowen, Aoife, O'Higgins, Amy C., Xu, Jun-Li, 2024. Advanced optical photothermal infrared spectroscopy for comprehensive characterization of microplastics from intravenous fluid delivery systems. Sci. Total Environ. 929, 172648. https://doi.org/10.1016/j.scitotenv.2024.172648.
Tarte, James V., Johir, Md Abu Hasan, Tra, Van-Tung, Cai, Zhengqing, Wang, Qilin, Nghiem, Long D., 2024. Optimising microplastics analysis for quantifying and identifying microplastic fibres in laundry wastewater. Sci. Total Environ. 952, 175907. https://doi.org/10.1016/j.scitotenv.2024.175907.
Vianello, Alvise, Jensen, Rasmus Lund, Liu, Li, Vollertsen, Jes, 2019. Simulating human exposure to indoor airborne microplastics using a breathing thermal manikin. Sci. Rep. 9 (1), 8670. https://doi.org/10.1038/s41598-019-45054-w.
Wedin, Helena, Niit, Ellinor, Mansoor, Zaheer Ahmad, Kristinsdottir, Anna Rúna, la Motte, de, Hanna, Jönsson, Christina, Lindgren, Christofer, 2018. Preparation of viscose fibres stripped of reactive dyes and wrinkle-free crosslinked cotton textile finish. J. Polym. Environ. 26 (9), 3603–3612. https://doi.org/10.1007/s10924-018-1239-y.
Wu, Lin Mei, Tong, Dong Shen, Zhao, Li Zhi, Yu, Wei Hua, Zhou, Chun Hui, Wang, Hao, 2014. Fourier transform infrared spectroscopy analysis for hydrothermal transformation of microcrystalline cellulose on montmorillonite. Appl. Clay Sci. 95, 74–82.
Xiao, Shuolin, Cui, Yuanfeng, Brahney, Janice, Mahowald, Natalie M., Li, Qi, 2023. Long-distance atmospheric transport of microplastic fibres influenced by their shapes. Nat. Geosci. 16 (10), 863–870. https://doi.org/10.1038/s41561-023-01264-6.
Yang, Haiping, Yan, Rong, Chen, Hanping, Lee, Dong Ho, Zheng, Chuguang, 2007. Characteristics of hemicellulose, cellulose and lignin pyrolysis. Fuel (Guildf.) 86 (12), 1781–1788. https://doi.org/10.1016/j.fuel.2006.12.013.
Zhang, Yulan, Kang, Shichang, Allen, Steve, Allen, Deonie, Gao, Tanguang, Sillanpää, Mika, 2020. Atmospheric microplastics: a review on current status and perspectives. Earth Sci. Rev. 203, 103118. https://doi.org/10.1016/j.earscirev.2020.103118.
Zhao, Xinran, Zhou, Yupeng, Liang, Chenzhe, Song, Jianchen, Yu, Siyun, Liao, Gengxuan, Wu, Chenmiao, 2023. Airborne microplastics: occurrence, sources, fate, risks and mitigation. Sci. Total Environ. 858, 159943. https://doi.org/10.1016/j.scitotenv.2022.159943.
Zhu, Xuan, Huang, Wei, Fang, Mingzhu, Liao, Zhonglu, Wang, Yiqing, Xu, Lisha, Shang, Xu, 2021. Airborne microplastic concentrations in five megacities of Northern and Southeast China. Environ. Sci. Technol. 55 (19), 12871–12881. https://doi.org/10.1021/acs.est.1c03618.